Applied Clay Science 215 (2021) 106300

Contents lists available at ScienceDirect

Applied Clay Science

journal homepage: www.elsevier.com/locate/clay

Research Paper

Multi-site nanocomposite sorbent for simultaneous removal of diverse micropollutants from treated wastewater

Ofri B. Zusman, Amir Perez, Yael G. Mishael *

Department of Soil and Water Sciences, The Robert H. Smith Faculty of Agriculture, Food, and Environment, Hebrew University of Jerusalem, Rehovot 7610001, Israel

ARTICLE INFO

Keywords:
Treated wastewater
Clay polymer nanocomposites
Micropollutants
Water filtration

ABSTRACT

Despite the advantages of maximizing treated wastewater (TWW) reuse, this practice brought upon the presence of micropollutants in edible plants, animals, and even humans, since many micropollutants are not completely removed by conventional treatment plants. Clay polymer nanocomposites (CPNs) have been proposed and widely studied in recent years as a promising sorbent for micropollutant removal. However, most of these studies report the development of a single CPN for the removal of specific micropollutants in batch experiments, usually from synthetic water, and do not compare to the removal by commercial sorbents. Here, we thoroughly investigated the adsorption mechanism of three chemically-diverse micropollutants; cationic, anionic, and non-ionic (metoprolol, diclofenac, and lamotrigine, respectively) from TWW by a CPN with a 'loopy' polymer configuration. The results suggest that both cation and anion exchange sites coexist on the CPN, and therefore anionic and cationic micropollutants adsorb simultaneously, and they do not compromise the adsorption of each other. The adsorption of the non-ionic micropollutant enhanced in the presence of the charged micropollutants due to a synergistic effect. These adsorption trends were also obtained for micropollutant filtration by CPN columns. Finally, we demonstrated the simultaneous filtration of effluent organic matter and an array of micropollutants from TWW by the CPN columns and compared it to the filtration by granular activated carbon (GAC). A cost-effective comparison indicates that the filtration by the CPN column is more efficient (ng pollutants/ sorbent cost) than by the GAC column.

1. Introduction

The reuse of treated wastewater (TWW) for agricultural irrigation, industrial processes and, even for human drinking dramatically increased over the past decades due to technological improvements (Gadipelly et al., 2014; Kosek et al., 2020; Meneses et al., 2010) and reduced treatment costs (Gupta et al., 2012; Muga and Mihelcic, 2008). Yet, most treatment plants fail to totally remove micropollutants and effluent organic matter (EfOM) from TWW, which may pose health issues. For example, the uptake of micropollutants such as pharmaceuticals by plants irrigated with TWW has been documented (Shenker et al., 2011; Eggen and Lillo, 2012; Wu et al., 2013; Gorovits et al., 2020). Although the concentrations of these contaminants are typically low (<1 μg/L), they may pose risks, especially if bioconcentrated by crops (Chefetz et al., 2008; Oulton et al., 2010; Siemens et al., 2008). A recent report demonstrated the association between elevated urine carbamazepine concentrations and consumption of daily recommended quantities of vegetables irrigated with TWW within adult and children populations (Schapira et al., 2020). Uncertainties about the risks associated with chronic exposure to chemicals in TWW and their possible additive or synergistic mixture effects raise serious concerns about water reuse. Consequently, a few countries, mainly Switzerland and Germany, began monitoring and regulating the concentrations of several micropollutants in their water sources and are currently considering technologies for micropollutant reduction (Kosek et al., 2020; Miarov et al., 2020). Conventional techniques include oxidation, advanced oxidation, nanofiltration, reverse osmosis, membrane bioreactor, and adsorption by sorbents (Couto et al., 2019; Khanzada et al., 2020; Schaar et al., 2010; Shin et al., 2021; Van Der Bruggen and Vandecasteele, 2003). One of the most common sorbents applied in filtration columns for the removal of organic micropollutants is granular activated carbon (GAC) (Benstoem et al., 2017). The extensive use of GAC is attributed to its high adsorption capacity, ability to adsorb a broad range of micropollutants with great efficacy due to its diverse pores size (Dąbrowski et al., 2005; Gur-Reznik et al., 2008; Moreno-Castilla, 2004; Namasivayam and Kavitha, 2002). Nevertheless, micropollutant adsorption efficiency is

* Corresponding author.
E-mail address: yael.mishael@mail.huji.ac.il (Y.G. Mishael).

https://doi.org/10.1016/j.clay.2021.106300
Received 20 May 2021; Received in revised form 29 September 2021; Accepted 1 October 2021
Available online 20 October 2021

dramatically compromised in the presence of EfOM associated with pore blockage (Aschermann et al., 2019; Newcombe et al., 1997; Zietzschmann et al., 2014). The removal of EfOM itself by GAC has many drawbacks, mainly a rapid decrease in sorbent efficiency (Benstoem et al., 2017; Chowdhury et al., 2013), requiring frequent expensive regeneration (Lambert et al., 2002; Sebastiani et al., 1994).

Clay polymer nanocomposites (CPNs) have been proposed and widely studied in recent years as an excellent alternative sorbent for micropollutant removal (Kohay et al., 2015; Levy et al., 2019; Medhat Bojnourd and Pakizeh, 2018; Mohd Amin et al., 2016; Shabtai et al., 2021; Unuabonah and Taubert, 2014). Few studies investigate the removal of an array of micropollutants by CPNs (Ray et al., 2019; Shabtai and Mishael, 2018) but usually they do not address the diverse driving adsorption mechanisms (Lozano-Morales et al., 2018; Mohd Amin et al., 2016) .A recent review suggests that more studies should rigorously evaluate novel CPNs for the removal of emerging pollutants at environmentally relevant concentrations and in realistic operational conditions (Shabtai et al., 2021). Indeed, most studies on CPNs report the development of a single CPN for the removal of specific micropollutants in batch experiments, usually from synthetic water (which do not include EfOM), and do not compare to the removal by commercial sorbents (Khodakarami and Bagheri, 2021; Shabtai et al., 2021).

Recently we reported the development of a novel CPN based on poly-4-vinylpyridine (PVP), 50% substituted with ethanol (OH50PVP), and its high affinity and rapid removal towards an anionic micropollutant (gemfibrozil) from TWW. The high affinity of gemfibrozil was explained in terms of more accessible adsorption sites on the polycation, due to its 'loops & tails' configuration (Levy et al., 2019). In the current study, we thoroughly investigated the adsorption mechanism of three chemically-diverse micropollutants, positively charged, negatively charged, and neutral from TWW, and identified different adsorption sites on the OH50PVP-CPN. Furthermore, we studied the simultaneous filtration of EfOM and an array of micropollutants from TWW by the CPN and GAC columns.

2. Materials and methods

2.1. Materials

Wyoming Na-montmorillonite SWy-2 (MMT) was obtained from the Source Clays Repository of the Clay Mineral Society (Columbia, MO). The cation exchange capacity (CEC) and nitrogen adsorption surface area of MMT are 76.4 cmol/kg and 31.82 m^2/g, respectively (Olphena and Fripiat, 2009). Poly-4-vinylpyridine (PVP, Mw-6000 Da), diclofenac sodium salt (pKa 4.15), metoprolol tartrate (pKa 9.67), (all >97% purity) 2-bromoethanol, ethanol, and all other reagents were purchased from Sigma Aldrich. Lamotrigine (pKa 5.71) (>99%) was purchased from EnzoBiochem Inc. (New York). Granular activated carbon (GAC) Hydraffin CC 8 × 30 (Donau Carbon) was obtained from Benchmark Technologies with a granulation (mesh) and total BET specific surface area of 0.6–2.36 mm and 1150 m^2/g, respectively. Treated wastewater post-ultra-filtration was sampled from the wastewater treatment plant in Nir Etzion, Israel (Table S1).

2.2. Methods

2.2.1. CPN preparation

Poly-4-vinylpyridine (PVP) was 50% (randomly) substituted with bromo-ethanol to synthesize OH50PVP, and this polymer was adsorbed to the MMT for composite fabrication according to our previous study (Levy et al., 2019). Briefly, MMT clay suspension (4.2 g/L, in 2 L) was added to OH50PVP solution (0.55 g/L, in 3 L), reaching a final concentration of 1.67 g clay/L and 0.33 g polymer/L. The clay-polycation suspension was stirred with a magnetic stirrer for 24 h and filtered through paper (15 μm) using a Büchner funnel. The absorbance of the polycation in the supernatants was measured using UV − Vis spectrophotometry (Thermo Scientific, Evolution 300, Waltham, MA) at a wavelength of 230 nm. A standard calibration curve was fitted, and the amount of polycation adsorbed was calculated accordingly.

2.2.2. CPN drying methods characterization

To test the effect of drying methods on the CPN properties, the filtered CPN was freeze-dried using a lyophilizer or dried in a 105 °C oven for 24 h. The dried composites were sieved to particle sizes in the ranges of 50-140 μm, 250-500 μm, and 1-2 mm.

The specific surface area (SSA) and pore volume (PV) of lyophilizer dried CPN (LD-CPN), and oven-dried CPN (OD-CPN) were measured by using the Brunauer–Emmett–Teller (BET) method (E20, P/N 05069 Rev. W, Quantachrome Instruments). The adsorbed gas was nitrogen (N2). The samples were degassed for two and a half hours under vacuum, in the temperature range between 40 °C and 120 °C, where every half hour the temperature increased by 20 °C. The basal (d_{001}-value) spacings of oriented OD-CPN, LD-CPN, and MMT were measured by X-ray diffraction (XRD). On a round glass slide, 1–2 mL of the suspension was placed and left to sediment (oriented sample) overnight. The basal spacing was measured using an X-ray diffractometer (Philips PW1830/3710/3020) with Cu KR radiation, λ = 1.526 Å. OD-CPN and LD-CPN microphotographs were recorded using a field emission scanning electron microscope (SEM) (JSM-7800F, JEOL, Japan) equipped with a secondary electron detector with an accelerating voltage of 3 keV.

2.2.3. Micropollutants and EfOM analysis

Spiked micropollutants, diclofenac (DCF), lamotrigine (LTG), and metoprolol (MET), were analyzed by HPLC (Agilent Technologies 1200 series) equipped with a diode-array detector (Table 2). HPLC column was Ascentis Express C18 for DCF and LTG, and XBridge Phenyl 3.5 μm for MET. The flow rate was 0.7 mL/min for LTG, 0.5 mL/min for DCF and 0.8 mL/min for MET. Measurements were carried out isocratically. DCF, LTG, and MET were detected at 275, 220, and 273 nm with a Limit of quantification (mg/L) of 0.05,0.05 and 1, respectively. The mobile phases were acetonitrile/acidic DDW (0.1% formic acid) 60/40, Phosphate buffer (pH 8, 0.025 M): ACN:MeOH = 57/18/25 and acetonitrile/acidic DDW (0.1% formic acid) 70/30 for DCF, LTG and MET, respectively.

Abundant of micropollutants in TWW solutions were analyzed by LC-MS, Agilent 1200 Rapid Resolution LC system (Agilent Technologies Inc., Santa Clara, CA) equipped with a Gemini C-18 column (150 × 2 mm, 3-μm particle size; Phenomenex, Torrance, CA, USA), coupled to an Agilent 6410 triple quadrupole mass spectrometer with an ESI ion source (Agilent). A binary gradient of 1.5% acetic acid in deionized water and 0.05% acetic acid in acetonitrile was used to separate the PCs.

EfOM was filtered through PTFE syringe filter (AXIVA) 0.45 μm pore size prior to measurement. UV–vis absorbance at a wavelength of 254 nm was measured with a spectrophotometer (Thermo Scientific, Evolution 300, Waltham, MA). Dissolved organic carbon (DOC) was determined using a VCSH total organic carbon analyzer (Shimadzu, Japan; detection limit was 0.5 mg C L^{-1}). In order to obtain specific ultraviolet absorption (SUVA), UV absorbance at 254 nm was divided by DOC concentration.

2.2.4. Micropollutant and EfOM adsorption at equilibrium

The effect of drying method on the adsorption was conducted by preparing stock solutions of TWW spiked with MET (200 mg/L), DCF, and LTG (1 mg/L each). These solutions and unspiked TWW (9.4 mg DOC/L) were added to Eppendorf tubes containing different particle sizes of OD-CPN or LD-CPN (1.92–3.84 g/L). The CPNs were resuspended, and the tubes were agitated for 24 h (reaching equilibrium). Supernatants were separated by centrifugation (10,000 RPM for 20 min), filtered with PTFE syringe filter (AXIVA) 0.45 μm pore size, and measured by HPLC and spectrophotometer. Tests indicated that there was no sorption by the filter. The experiments were performed in triplicate, and samples were kept in darkness to avoid photodegradation.

The adsorption isotherms experiments were performed by adding MET (25–700 mg/L), LTG (0.4–20 mg/L), and DCF (0.5–30 mg/L) to Eppendorf tubes containing medium size particles of LD-CPNs (1.9 g/L, 7.68 g/L, and 0.95 g/L, respectively) or MMT (1.7 g/L, 6.68 g/L, and, 0.84 g/L respectively). The adsorption experiment procedures and measurements were performed as described above. Using nonlinear regression with GraphPad Prism 5, the results were tested to fit the Langmuir and the Freundlich models. Langmuir: $q_e = \frac{Q_{max} K\ C_e}{1+K\ C_e}$, where q_e is the concentration of contaminant added in equilibrium (mg/g), C_e is the concentration of the contaminant at equilibrium in the solution (mmol/L), Q_{max} is the maximum adsorbent surface sites (mmol/g).

Freundlich: K is Langmuir constant (L/mmol), k_f is Freundlich constant, and n is a correction factor. $q_e = k_f C_e^{1/n}$.

To study the effect of competition, two micropollutants were added at equal concentrations (2 mg/L) to the same solution, i.e., three combinations were tesetd (MET+LTG, DCF + MET, LTG + DCF). The solutions were added to Eppendorf tubes containing OH50PVP CPN (1.92 g/L), and the adsorption experiment procedures and measurements were performed as described above.

2.2.5. Micropollutant and EfOM Filtration

All filtration experiments were conducted in duplicates with glass columns (20 cm length, 1 cm diameter, 5 mL pore volume), containing 1 g of sorbent (OH50PVP CPN or GAC) mixed with 20 g of quartz sand (0.8–1.5 mm). Columns washed first with 500 mL DW to thrust any possible dirtiness. Three separate stock solutions of TWW spiked with MET (5 mg/L) LTG (1 mg/L) and DCF (1 mg/L), prepared and pumped through the columns at a flow rate of 1.5 mL/min. Samples were filtered with PTFE syringe filter (AXIVA) 0.45 μm pore size prior to HPLC analysis.

In addition, simultaneous filtration of TWW spiked with the three micropollutants, MET (5 mg/L) LTG (1 mg/L) and DCF (1 mg/L), prepared and pumped through the columns at a flow rate of 1.5 mL/min. The effluent of the columns was collected with time, and the concentrations of the micropollutant and of the EfOM were measured as described above.

3. Results and discussion

3.1. Effect of CPN drying mode on its physical properties

CPN drying mode, oven vs. lyophilizer, must have an immense effect on CPN physical properties, including pore size distribution. While the effect of GAC pore size on the adsorption capacity and kinetic of molecules as a function of their molecular weight has been reported (Kilduff et al., 1996; Piai et al., 2019; Schreiber et al., 2005; Valderrama et al., 2008), the effect of CPN pore size on adsorption is rarely addressed (Zusman et al., 2020). EfOM and micropollutants have a broad range of molecular weights, therefore we characterized oven-dried CPN (OD-CPN) and lyophilizer-dried CPN (LD-CPN) employing BET (total pore volume mm^3/g), SEM (micro-pores), and XRD (nano-pores) (Fig. 1).

The surface area of LD-CPN, at different particle sizes, small (50-140 μm), medium (250-500 μm), and large (1-2 mm), was higher than the OD-CPN with the same particle size, by 130%, 320%, and 480%,

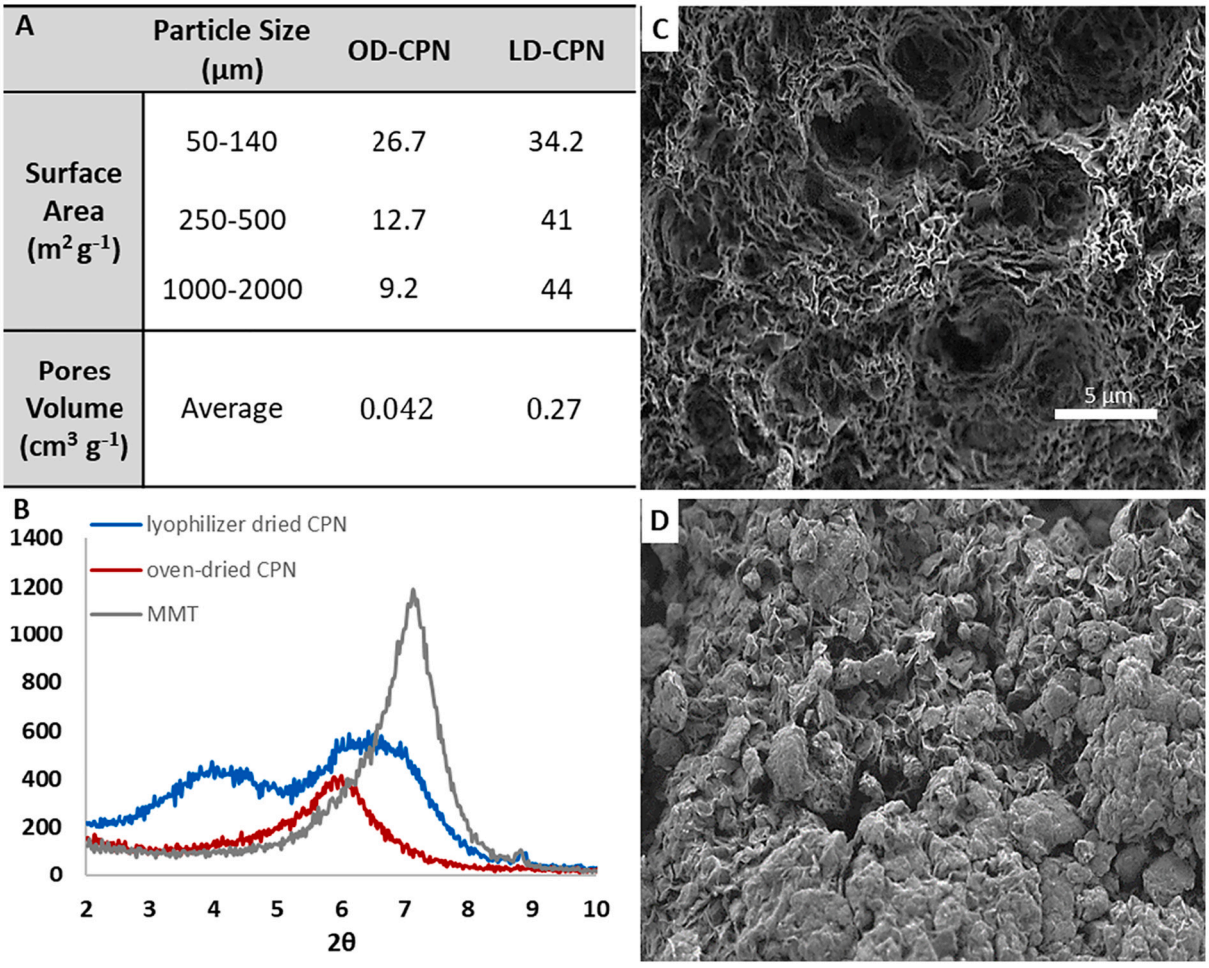

Fig. 1. Characterization of OD-CPN and LD-CPN. (A) BET [surface area ± 0.15 m^2/g, pore volume ± 0.02 cm^3/g], (B) X-Ray diffraction, and (C, D) SEM images of LD-CPN and OD-CPN, respectively.

respectively. The average pore volume of LD-CPN is one order of magnitude higher than that of OD-CPN (Fig. 1A). The higher surface area and pore volume of LD-CPN and OD-CPN can be explained by the water exclusion mechanism during the drying process. In oven drying, water molecules are removed by evaporation which creates high pressure on the pores and results in pore collapse. In contrast, the freezing drying process is based on the sublimation of water molecules, which induces small pressure on the pores, and therefore they remain intact (Thompson et al., 1985).

These different water exclusion mechanisms, may also explain why particle size had a minor effect on the surface area for the LD-CPNs, while for the OD-CPNs, an increase in surface area was obtained as particle size decreases. The smaller OD-CPN particles have a surface area of nearly 3-fold higher than the surface area of the large particle, 26.7 and 9.2 m^2/g, respectively. Such a trend is expected when the external surface area is dominant, however, if the degree of the internal surface area is high, the effect of particle size on the surface area would not be pronounced, as observed in the case of the LD-CPNs.

At a lower scale (micron), we can also identify that the LD-CPNs have a more porous structure than the OD-CPNs based on SEM images (Fig. 2C-D). The differences between LD-CPN and OD-CPN were not only observed at the micron scale but also at the platelet-platelet scale (nm) (Fig. 1B). A basal spacing of 12.2 Å was obtained for MMT by XRD measurements. In the OD-CPN diffractogram, one peak was observed at 14.6 Å, while in the LD-CPN diffractogram, two broad peaks were observed at the range of 12.5–14.6 Å and 19–24 Å. The basal spacings of 14.6 Å and 12–14.6 Å, for OD-CPN and LD-CPN, respectively, can be related to polymer intercalation in a 'train' configuration (ref.) whereas the 19–24 Å basal spacing, found only in LD-CPN, can be related to polymer intercalation in a more extended configuration such as 'loops & tails' as we have previously reported (Levy et al., 2019). Additional studies have also suggested that CPN diffractions at low angles can be attributed to a polymer configuration of 'loops & tails' (Churchman, 2002; Radian and Mishael, 2008). In the OD-CPN diffractogram, this peak at low angles does not appear, perhaps water evaporation during the oven drying brings upon pore and polymer structural collapse.

3.2. The effect of CPN drying mode on DCF, LTG, and MET removal

In order to test the effect of CPN pore size on the adsorption efficiency, DCF, LTG, and MET, with molecular weights of 250–300 g/mol and EfOM, a group of molecules with an extremely broad range of molecular weights (Nam and Amy, 2008; Shon et al., 2006; Yu et al., 2012), were adsorbed to OD-CPN and LD-CPN with increasing particle size (Fig. 2).

The removal by LD-CPNs was dramatically higher than the removal by OD-CPNs. For EfOM the removal was three times higher by the small LD-CPNs particles and one order of magnitude higher by the large particles. The adsorption of DCF, LTG and, MET by LD-CPNs was also significantly higher than OD-CPN, for example, the removal by medium-size particle LD-CPN was 2, 1.8 and, 1.5 times higher, respectively. For the OD-CPNs, micropollutant removal increased as particle size

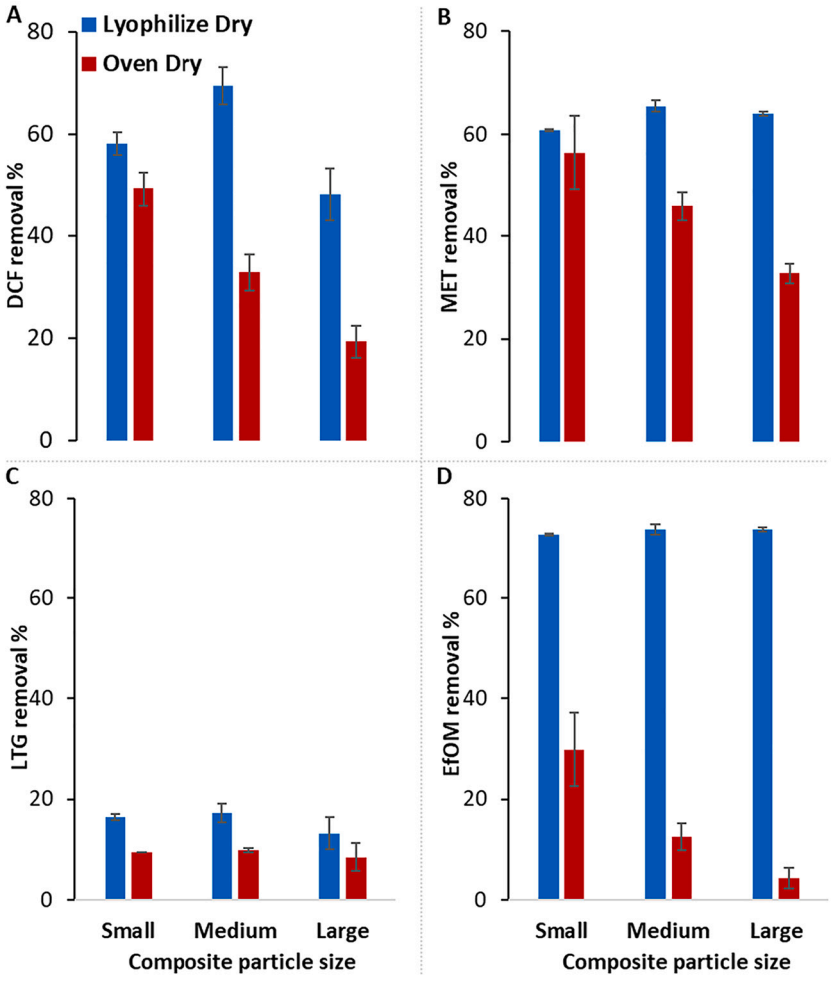

Fig. 2. Removal of (A) DCF (1 mg/L), (B) MET (200 mg/L), (C) LTG (1 mg/L), and (D) EfOM (9 mg/L) from TWW, by lyophilized and oven dried CPNs with particle sizes of small (50–140 μm), medium (250–500 μm), and large (1000–2000 μm).

decreased, while, for the LD-CPNs, the removal was not affected by particle size, correlating with particle surface area trends. Specifically, no differences in removal were obtained for LTG, even for the OD-CPNs, due to its extremely low removal.

LTG (1 mg/L), a non-ionic micropollutant, removal was also extremely low by the LD-CPNs (~20%), while the cationic MET removal was high (~80%) despite its relatively high initial concentration (200 mg/L), and the removal of the anionic micropollutant, DCF (1 mg/L), also reached ~80% removal. To further explore these trends, adsorption isotherms of the three micropollutants to unmodified MMT and to the LD-CPN (medium size particles), were obtained (Fig. 3A-C), and adsorption coefficients were extracted (Fig. 3D).

3.3. DCF, LTG and MET adsorption to CPN and MMT

The adsorption isotherms of MET and DCF well fit the Langmuir model while LTG isotherms well fit to the Freundlich model (Fig. 3D). The adsorption of the micropollutants to the unmodified-MMT was as expected, i.e., negligible for DCF and LTG due to chemical repulsion and weak attraction, respectively, and very high for MET due to strong electrostatic attraction. The adsorption of MET to the OH50PVP CPN was an order of magnitude higher than DCF and two orders of magnitude than LTG (Fig. 3A-C).

For LTG, the Freundlich 1/n coefficient was nearly one, a linear equation, suggesting a partition mechanism generally attributed to the attraction between relatively non-polar molecules to non-specific binding sites, particularly by van-der Walls bonds. Supporting this result, we performed an additional adsorption test, in which LTG concentration was constant (2 mg/L) while increasing the OH50PVP CPN concentration (1.9–15.2 g/L) and the trend remained linear (Fig. S1).

The higher adsorption of DCF to the OH50PVP CPN (Qmax = 0.04 mmol/g), in comparison to the unmodified-MMT, was attributed to the electrostatic attraction between the anionic DCF and the positively charged composite (Levy et al., 2019). DCF affinity constant (K) to the OH50PVP CPN was high 23.4 L/mmol, compared to the negligible affinity to unmodified-MMT, indicating DCF adsorption to the OH50PVP CPN was to the polymer component. Identical DCF adsorption coefficients to a CPN with a similar polymer were obtained (Kohay et al., 2015). Accordingly, the affinity of the cationic MET to the OH50PVP CPN is relatively low (10 L/mmol) due to electrostatic repulsion.

MET adsorption capacity to the unmodified-MMT reached 80% of the clay's CEC (0.6 of 0.76 mmol/g). Despite the positive zeta potential of the OH50PVP CPN (+50 mV) MET adsorption capacity was high (0.3 mmol/g), indicating that at least 0.3 mmol/g are not occupied by the polycation. Although the polycation loading in the CPN is extremely high (1.33 mmol/g) (Levy et al., 2019), a maximum of 0.44 mmol sites/g are occupied by the polycation. This observation further supports our previous conclusion that OH50PVP adsorbs on MMT in a 'loopy' configuration (Levy et al., 2019). MET adsorption capacity to the OH50PVP CPN was higher than the adsorption capacity of the anionic DCF to the OH50PVP CPN (0.04 mmol/g), suggesting that both cation and anion exchange sites coexist on the OH50PVP CPN with a magnitude higher amount of cation exchange capacity sites (due to MMT sites).

MET adsorption to the OH50PVP CPN was very high, 0.3 mmol/g, suggesting its intercalation between the clay platelets. To verify MET intercalation, XRD measurements of unmodified-MMT, OH50PVP CPN, MET adsorbed on unmodified-MMT, and MET adsorbed on OH50PVP CPN, were performed (Fig. 3E). MET adsorption to the clay (0.6 mmol/g) increased the basal spacing from 12.2 Å (one layer of water) to 14.8 Å, indicating MET adsorbed between the platelets. The OH50PVP CPN has two peaks, at 12.5–14.6 Å and 19–24 Å, attributed to polycation intercalation as train and as loops & tails, respectively (Fig. 1B). Upon MET adsorption to the OH50PVP CPN, the 19–24 Å peak appears, the peak at 12.5–14.6 Å does not appear, but an additional peak appears at 14.8 Å as obtained for the MET-MMT complex. To explain this phenomenon, we hypothesize that upon the adsorption of 40% of the CEC by the cationic MET (adsorption coefficient 10.01 L/mmol) it may thrust the polycation adsorbed as trains (adsorption coefficient of 9 L/mmol (Levy et al., 2019)) but less likely thrusts the polycation adsorbed as loops & tails (adsorption coefficient 24 L/mmol (Levy et al., 2019)). Micropollutants may intercalate between CPN platelets without thrusting the polycation

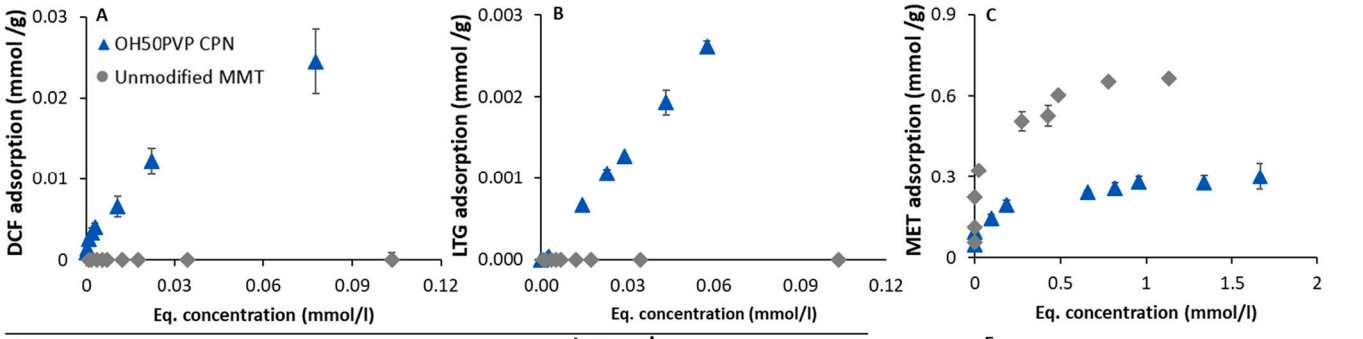

D

Pollutants	Sorbent	Langmuir Q max (mmol/g)	Langmuir K (L/mmol)	Langmuir R^2
MET	Composite	0.30	10.01	0.82
	Clay	0.61	46.91	0.83
DCF	Composite	0.04	23.24	0.97
	Clay	0	0	
		Freundlich K_f (L g/mmol)	Freundlich 1/n	Freundlich R^2
LTG	Composite	0.04	0.99	0.99
	Clay	0	0	

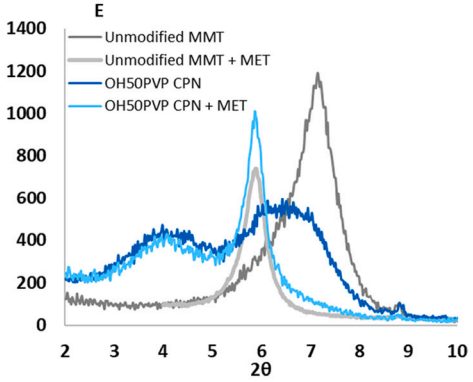

Fig. 3. Adsorption isotherms of (A) DCF (0.25–30 mg/L) (B) LTG (0.4–20 mg/L) and (C) MET (25–700 mg/L) to unmodified MMT (0.8–1.7 g/L) and OH50PVP CPN (1–2 g/L), (D) Adsorption coefficients, (E) MMT and OH50PVP CPN XRD diffractogram prior and upon MET adsorption.

as reported for DCF, which adsorbed to the intercalated quarternized poly vinyl- pyridinium-*co*-styrene (QPVPcS) (very similar chemical structure to OHPVP) (Kohay et al., 2019).

3.4. DCF, LTG, and MET simultaneous adsorption by CPN – batch experiments

To conclude, based on the adsorption isotherms, we suggest that MET and DCF adsorb with relatively high affinity to the unmodified MMT surface and to the OH50PVP CPN, respectively, due to electrostatic interactions. LTG adsorption is negligible to the unmodified MMT and has low affinity and capacity to the OH50PVP CPN. To reinforce these conclusions that molecules with different chemical properties adsorb to different sites, MET, DCF, and LTG adsorption in competition was conducted, i.e., simultaneous adsorption of two molecules (Table 1). The removal of MET was not compromised in the presence of DCF or LTG, however, the removal of DCF and LTG was affected by competition. MET has a high affinity to the CEC sites of the clay, which are not relevant for DCF and LTG, and therefore its removal was not compromised. DCF adsorbs with high affinity to the polycation component therefore, we hypothesized that the presence of LTG (low affinity to the polycation) or MET (does not adsorb to the polycation) would not affect its removal. Indeed, LTG had a slight effect on DCF removal, however, DCF removal significantly enhanced in the presence of MET. MET screens the local negative surface charge of MMT and may even bring upon a local positive charge, which obviously enhances DCF removal.

Surprisingly, compared to the low removal without competition (10%), LTG removal increased moderately in the presence of MET (36%) and dramatically in the presence of DCF (85%). The results can be explained by a synergistic adsorption mechanism. Adsorption of positively charged molecules to the negative clay surface, or alternatively, adsorption of negatively charged molecules to the positive polycation, screens the local charges and therefore enhances the adsorption of lipophilic molecules, such as LTG, to the polymer and the MMT through hydrophobic interaction.

3.5. DCF, LTG, and MET simultaneous adsorption by CPN and GAC – filtration experiments

The adsorption capacities and affinities of MET, DCF, and LTG to the OH50PVP CPN were determined, and various adsorption mechanisms were suggested based on equilibrium experiments. To further test the suggested mechanisms, we examined the effect of separate and simultaneous filtration of the three micropollutants spiked to TWW by an OH50PVP CPN and GAC columns (Fig. 4).

The filtration efficiency of the micropollutants by the OH50PVP CPN columns correlated with the trends observed from the adsorption isotherms. The removal of MET by filtration with the OH50PVP CPN column was complete throughout the entire experiment, while the removal by the GAC column decreased from 95 to 86%. The filtration of MET by the OH50PVP CPN column was not compromised in the presence of DCF and LTG (Fig. 4C). The removal of DCF by the OH50PVP CPN column was complete throughout the first 20 PV and decreased to 50% at the end of the experiment (110 PV), whereas the removal by the GAC column decreased to 55% after 60 PV. Similar to the equilibrium study, the removal of DCF slightly improved in the presence of LTG and MET (Fig. 4A). As mentioned above, we suggested (based on the equilibrium studies) that the LTG adsorption is mainly via hydrophobic interactions. Indeed its filtration by GAC, a well-known hydrophobic sorbent, is extremely high. The filtration of LTG by the OH50PVP CPN column was extremely enhanced in the presence of MET and DCF (Fig. 4B), reinforcing the suggested synergistic effect obtained from the equilibrium studies.

Table 1
Adsorption of MET, DCF and LTG (2 mg/L) by OH50PVP CPN (2 g/L).

Target pollutant	In the presence of	Removal of target pollutant (%)
MET	MET	100
	DCF	100
	LTG	100
DCF	MET	78 ± 0.6
	DCF	57 ± 7.5
	LTG	72 ± 6
LTG	MET	36 ± 0.6
	DCF	85 ± 0.25
	LTG	10 ± 0.13

3.6. Multimicropollutant filtration from TWW

Finally, the efficiency of treating TWW by OH50PVP CPN columns was demonstrated by studying the simultaneous filtration of several abundant micropollutants and EfOM and comparing it to the filtration by GAC columns (Fig. 5-6).

The micropollutant concentrations ranged from 12 ng/l (Bezafibrate) to 1475 ng/l (Carbamazepine), while EfOM concentration was four orders of magnitude higher, 9 g/l.

Micropollutant removal by filtration within 30 min (Fig. 5A) and 90 min (Fig. S2) by the OH50PVP CPN and GAC columns was high by at least one sorbent for most pollutants. LTG, DCF, and MET were adsorbed by the OH50PVP CPN with 30, 90, and 100% removal, respectively, roughly following the trends obtained in this study.

From an economic and applicable point of view, the removal of micropollutants per sorbent price (ng pollutants/ sorbents price) indicates the productivity of the sorbents (Fig. 5B). The average price of GAC is ~0.56 cent/g (Alhashimi and Aktas, 2017; Paredes et al., 2018), while the composite unit price is ~0.115 cent/g (table S2). The filtration of all micropollutants by the OH50PVP CPN column (ng pollutants/ cent sorbent) was much higher than by the GAC column. The total removal by OH50PVP CPN and by GAC reached 1938 vs. 555 ng pollutants/cent sorbent, expressing the cost-effective advantage of the OH50PVP CPN.

3.7. EfOM filtration from TWW

Despite the high interest in micropollutant removal, the real challenge in treating TWW is the coexisting of diverse micropollutants with EfOM, with a concentration of three to six orders of magnitude higher. Therefore, demonstrating the high removal of EfOM by the developed CPN is essential (Fig. 6).

EfOM removal by filtration with the OH50PVP CPN column, throughout the entire experiment, was almost twice that of the GAC column when measured by UV_{254}, while the removal efficiency of the sorbents was equal, reaching ~60% when DOC was measured (Fig. 6A). These results indicate selective adsorption by the sorbents and attraction of different fractions from the EfOM. To further demonstrate that different EfOM components are attracted by different sorbents, the specific ultraviolet absorption (SUVA) was calculated at the inlet and the outlet of the columns (Fig. 6B). SUVA is strongly correlated with the aromaticity of the organic matter compound and describes the nature of EfOM in the water in terms of hydrophobicity and hydrophilicity (Edzwald and Tobiason, 1999; Matilainen et al., 2011). The inlet SUVA was 1.8, and post-filtration through the OH50PVP CPN column, the SUVA decreased to 1.4, suggesting that dissolved humic substances (the main contribution to the bulk EfOM UV absorption) mainly adsorbed, whereas, upon filtration through GAC columns, the SUVA increased to 3, suggesting that dissolved humic substances did not adsorb. The same trend, decrease and increase in SUVA values upon filtration with positively charged CPN and with GAC, respectively, were reported in our previous study on surface water (Zusman et al., 2020). The reduction of dissolved humic substances is essential because it one of the fractions related to disinfection by-products formation and biofilm generation. From an economic point of view, the total removal of EfOM by

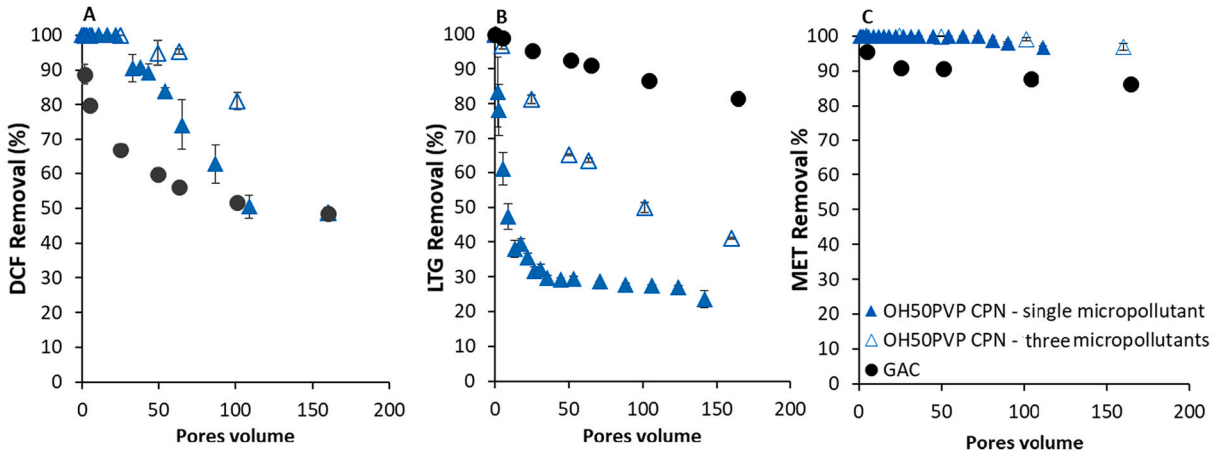

Fig. 4. Filtration of (A) DCF (1 mg/L), (B) LTG (1 mg/L), and (C) MET (5 mg/L), from TWW spiked with a single or with the three micropollutants by OH50PVP CPN and GAC columns (mix with sand with 1:20 ratio).

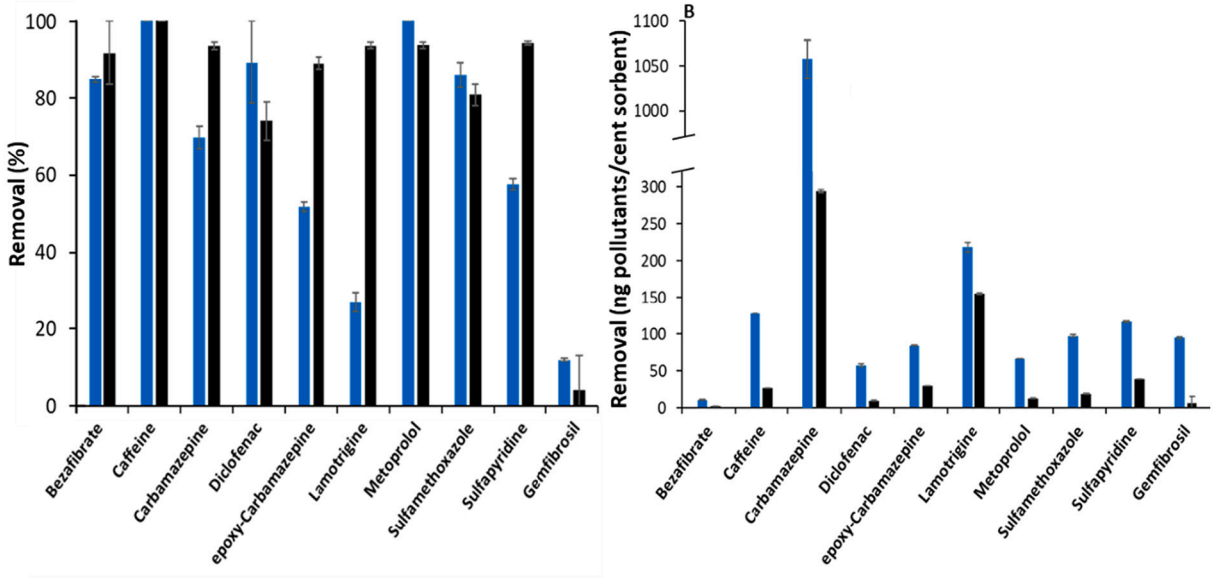

Fig. 5. Filtration of micropollutants (0.01–2 μg/L) from TWW within 30 min by OH50PVP-CPN and GAC column (mix with sand 1:20 *w*/w). Removal of micropollutants (A) percent of inlet concentration removed by column (%), (B) weight of micropollutant removed per gram sorbent (ng/g) divided by sorbent price (cent/g sorbent).

OH50PVP CPN and by GAC reached 10 vs. 50 g EfOM/cent sorbent, expressing the cost-effective advantage of the OH50PVP CPN.

4. Conclusion

Simultaneously removing a wide range of micropollutants at low concentrations is challenging, but the presence of relatively high EfOM concentrations in TWW further increases the complexity of the goal. To overcome these challenges, a multi-site CPN sorbent with a 'loopy' polycation structure was selected, and the adsorption of three chemically diverse micropollutants, MET (positive), DCF (negative), and LTG (neutral), was studied. The adsorption affinities of the micropollutants to the positively charged CPN (zeta potential 50 mV) correlated to their chemical properties DCF > MET>LTG, surprising the capacity of the positively charged micropollutant, MET, was extremely high and even higher than the negatively charged micropollutant, DCF. Based on the adsorption isotherms of each micropollutant to the unmodified MMT and the CPN and based on XRD measurements, we suggest that both MET and DCF adsorbed both on the external surface and between the CPN clay platelets. While DCF adsorbed to the 'loopy' polycation, MET adsorbs directly to the unmodified MMT and even partially excludes adsorbed polycation monomers from the clay surface. Despite the high interest in micropollutant removal, reduction in EfOM concentrations is just as important. Indeed, we demonstrated the successful simultaneous filtration of EfOM and an array of micropollutants from TWW by the CPN columns and compared them to the filtration by GAC columns. The filtration of the micropollutants and EfOM by the CPN column was more cost-effective (total removal /sorbent price) in comparison to the GAC column. Although the EfOM removal, measured via TOC, by both the CPN and GAC columns reached the same value (60%), the removal, measured via UV $_{254}$, was higher by the CPN column, indicating that the CPN adsorbs dissolved humic substances (the main contribution to bulk EfOM UV absorption) with high efficiency. Dissolved humic substance reduction is essential because it one of the fractions related to disinfection by-products formation and biofilm generation.

TWW is an extremely complex medium containing an enormous amount of different micropollutants and EfOM, making the understanding of the adsorption driving forces challenging. Looking at only

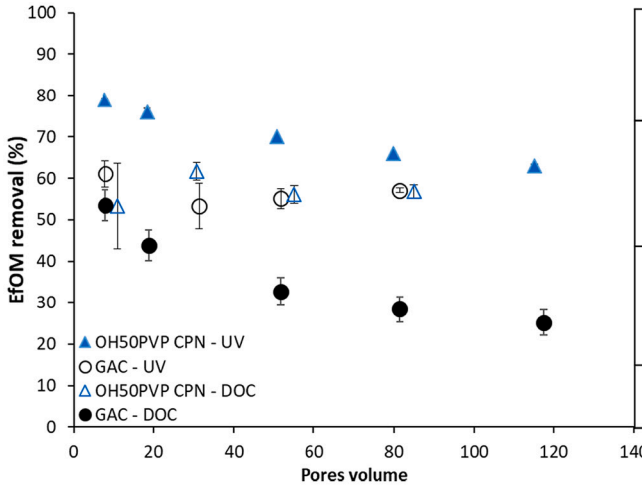

	Control	OH50PVP-CPN	GAC
Absorbance (UV 254)	0.23	0.08	0.17±0.007
TOC (g/L)	12.92	5.6±0.22	5.5±0.07
SUVA	1.8	1.4±0.05	3.1±0.09

Fig. 6. (A) Filtration of EfOM (9.4 g/L) from TWW by OH50PVP-CPN and GAC columns [mix with sand 1:20 w/w)] calculated by measuring UV absorption at 254 nm and by DOC content, (B) SUVA values calculated from filtration results (at 80 pore volume).

three models micropollutant to reach an in-depth understanding of the entire system may be somewhat simplistic. Experimentally studying the removal of hundreds of molecules from TWW is not feasible and perhaps a modeling approach is necessary.

Declaration of Competing Interest

The authors declare that they have no known competing financial interests or personal relationships that could have appeared to influence the work reported in this paper.

Acknowledgment

Supported by the Israeli Ministry of Science, Technology and Space #821-0142-06

Appendix A. Supplementary data

Supplementary data to this article can be found online at https://doi.org/10.1016/j.clay.2021.106300.

References

Alhashimi, H.A., Aktas, C.B., 2017. Life cycle environmental and economic performance of biochar compared with activated carbon: a meta-analysis. Resour. Conserv. Recycl. 118, 13–26. https://doi.org/10.1016/j.resconrec.2016.11.016.

Aschermann, G., Neubert, L., Zietzschmann, F., Jekel, M., 2019. Impact of different DOM size fractions on the desorption of organic micropollutants from activated carbon. Water Res. 161, 161–170. https://doi.org/10.1016/J.WATRES.2019.05.039.

Benstoem, F., Nahrstedt, A., Boehler, M., Knopp, G., Montag, D., Siegrist, H., Pinnekamp, J., 2017. Performance of granular activated carbon to remove micropollutants from municipal wastewater—a meta-analysis of pilot- and large-scale studies. Chemosphere. https://doi.org/10.1016/j.chemosphere.2017.06.118.

Chefetz, B., Mualem, T., Ben-Ari, J., 2008. Sorption and mobility of pharmaceutical compounds in soil irrigated with reclaimed wastewater. Chemosphere 73, 1335–1343. https://doi.org/10.1016/j.chemosphere.2008.06.070.

Chowdhury, Z., Summers, R., Westeroff, G., Leto, B., Nowac, K., Corwin, C., 2013. Activated carbon: solutions for improving water quality. Am. Water Work Assoc. https://doi.org/10.1002/0471238961.0103200902011105.a01.pub2.

Churchman, G.J., 2002. Formation of complexes between bentonite and different cationic polyelectrolytes and their use as sorbents for non-ionic and anionic pollutants. Appl. Clay Sci. 21, 177–189. https://doi.org/10.1016/S0169-1317(01)00099-0.

Couto, C.F., Lange, L.C., Amaral, M.C.S., 2019. Occurrence, fate and removal of pharmaceutically active compounds (PhACs) in water and wastewater treatment plants—a review. J. Water Process Eng. https://doi.org/10.1016/j.jwpe.2019.100927.

Dąbrowski, A., Podkościelny, P., Hubicki, Z., Barczak, M., 2005. Adsorption of phenolic compounds by activated carbon—a critical review. Chemosphere 58, 1049–1070. https://doi.org/10.1016/j.chemosphere.2004.09.067.

Edzwald, J.K., Tobiason, J.E., 1999. Enhanced coagulation: US requirements and a broader view. Water Sci. Technol. 40, 63–70. https://doi.org/10.1016/S0273-1223(99)00641-1.

Eggen, T., Lillo, C., 2012. Antidiabetic II drug metformin in plants: Uptake and translocation to edible parts of cereals, oily seeds, beans, tomato, squash, carrots, and potatoes. J. Agric. Food Chem. 60, 6929–6935. https://doi.org/10.1021/jf301267c.

Gadipelly, C., Pérez-González, A., Yadav, G.D., Ortiz, I., Ibáñez, R., Rathod, V.K., Marathe, K.V., 2014. Pharmaceutical industry wastewater: Review of the technologies for water treatment and reuse. Ind. Eng. Chem. Res. https://doi.org/10.1021/ie501210j.

Gorovits, R., Sobol, I., Akama, K., Chefetz, B., Czosnek, H., 2020. Pharmaceuticals in treated wastewater induce a stress response in tomato plants. Sci. Rep. 10, 1–13. https://doi.org/10.1038/s41598-020-58776-z.

Gupta, V.K., Ali, I., Saleh, T.A., Nayak, A., Agarwal, S., 2012. Chemical treatment technologies for waste-water recycling - An overview. RSC Adv. https://doi.org/10.1039/c2ra20340e.

Gur-Reznik, S., Katz, I., Dosoretz, C.G., 2008. Removal of dissolved organic matter by granular-activated carbon adsorption as a pretreatment to reverse osmosis of membrane bioreactor effluents. Water Res. 42, 1595–1605. https://doi.org/10.1016/j.watres.2007.10.004.

Khanzada, N.K., Farid, M.U., Kharraz, J.A., Choi, J., Tang, C.Y., Nghiem, L.D., Jang, A., An, A.K., 2020. Removal of organic micropollutants using advanced membrane-based water and wastewater treatment: a review. J. Membr. Sci. https://doi.org/10.1016/j.memsci.2019.117672.

Khodakarami, M., Bagheri, M., 2021. Recent advances in synthesis and application of polymer nanocomposites for water and wastewater treatment. J. Clean. Prod. https://doi.org/10.1016/j.jclepro.2021.126404.

Kilduff, J.E., Karanfil, T., Weber, W.J., 1996. Competitive interactions among components of humic acids in granular activated carbon adsorption systems: Effects of solution chemistry. Environ. Sci. Technol. 30, 1344–1351. https://doi.org/10.1021/es950546z.

Kohay, H., Izbitski, A., Mishael, Y.G., 2015. Developing polycation-clay sorbents for efficient filtration of diclofenac: effect of dissolved organic matter and comparison to activated carbon. Environ. Sci. Technol. 49, 9280–9288. https://doi.org/10.1021/acs.est.5b01530.

Kohay, H., Bilkis, I.I., Mishael, Y.G., 2019. Effect of polycation charge density on polymer conformation at the clay surface and consequently on pharmaceutical binding. J. Colloid Interface Sci. 552, 517–527. https://doi.org/10.1016/j.jcis.2019.05.079.

Kosek, K., Luczkiewicz, A., Fudala-Książek, S., Jankowska, K., Szopińska, M., Svahn, O., Tränckner, J., Kaiser, A., Langas, V., Björklund, E., 2020. Implementation of advanced micropollutants removal technologies in wastewater treatment plants (WWTPs) - examples and challenges based on selected EU countries. Environ. Sci. Pol. https://doi.org/10.1016/j.envsci.2020.06.011.

Lambert, S.D., Miguel, G.S., Graham, N.J.D., 2002. Deleterious effects of inorganic compounds during thermal regeneration of GAC: a review. J. Am. Water Works Assoc. 94, 109–119. https://doi.org/10.1002/j.1551-8833.2002.tb10253.x.

Levy, L., Izbitski, A., Mishael, Y.G., 2019. Enhanced gemfibrozil removal from treated wastewater by designed "loopy" clay-polycation sorbents: effect of diclofenac and effluent organic matter. Appl. Clay Sci. 182, 105278. https://doi.org/10.1016/j.clay.2019.105278.

Lozano-Morales, V., Gardi, I., Nir, S., Undabeytia, T., 2018. Removal of pharmaceuticals from water by clay-cationic starch sorbents. J. Clean. Prod. 190, 703–711. https://doi.org/10.1016/j.jclepro.2018.04.174.

Matilainen, A., Gjessing, E.T., Lahtinen, T., Hed, L., Bhatnagar, A., Sillanpää, M., 2011. An overview of the methods used in the characterisation of natural organic matter (NOM) in relation to drinking water treatment. Chemosphere 83, 1431–1442. https://doi.org/10.1016/j.chemosphere.2011.01.018.

Medhat Bojnourd, F., Pakizeh, M., 2018. Preparation and characterization of a nanoclay/PVA/PSf nanocomposite membrane for removal of pharmaceuticals from water. Appl. Clay Sci. 162, 326–338. https://doi.org/10.1016/j.clay.2018.06.029.
Meneses, M., Pasqualino, J.C., Castells, F., 2010. Environmental assessment of urban wastewater reuse: treatment alternatives and applications. Chemosphere 81, 266–272. https://doi.org/10.1016/j.chemosphere.2010.05.053.
Miarov, O., Tal, A., Avisar, D., 2020. A critical evaluation of comparative regulatory strategies for monitoring pharmaceuticals in recycled wastewater. J. Environ. Manag. 254, 109794. https://doi.org/10.1016/j.jenvman.2019.109794.
Mohd Amin, M.F., Heijman, S.G.J., Rietveld, L.C., 2016. Clay-starch combination for micropollutants removal from wastewater treatment plant effluent. Water Sci. Technol. 73, 1719–1727. https://doi.org/10.2166/wst.2016.001.
Moreno-Castilla, C., 2004. Adsorption of organic molecules from aqueous solutions on carbon materials. Carbon N. Y. 42, 83–94. https://doi.org/10.1016/j.carbon.2003.09.022.
Muga, H.E., Mihelcic, J.R., 2008. Sustainability of wastewater treatment technologies. J. Environ. Manag. 88, 437–447. https://doi.org/10.1016/j.jenvman.2007.03.008.
Nam, S.N., Amy, G., 2008. Differentiation of wastewater effluent organic matter (EfOM) from natural organic matter (NOM) using multiple analytical techniques. Water Sci. Technol. 57, 1009–1015. https://doi.org/10.2166/wst.2008.165.
Namasivayam, C., Kavitha, D., 2002. Removal of Congo Red from water by adsorption onto activated carbon prepared from coir pith, an agricultural solid waste. Dyes Pigments 54, 47–58. https://doi.org/10.1016/S0143-7208(02)00025-6.
Newcombe, G., Drikas, M., Hayes, R., 1997. Influence of characterised natural organic material on activated carbon adsorption: II. Effect on pore volume distribution and adsorption of 2-methylisoborneol. Water Res. 31, 1065–1073. https://doi.org/10.1016/S0043-1354(96)00325-9.
Olphena, H.V., Fripiat, J.J., 2009. Physical and Chemical Data of Source Clays [WWW Document] (Clay Clay Miner).
Oulton, R.L., Kohn, T., Cwiertny, D.M., 2010. Pharmaceuticals and personal care products in effluent matrices: a survey of transformation and removal during wastewater treatment and implications for wastewater management. J. Environ. Monit. 12, 1956–1978. https://doi.org/10.1039/c0em00068j.
Paredes, L., Alfonsin, C., Allegue, T., Omil, F., Carballa, M., 2018. Integrating granular activated carbon in the post-treatment of membrane and settler effluents to improve organic micropollutants removal. Chem. Eng. J. 345, 79–86. https://doi.org/10.1016/j.cej.2018.03.120.
Piai, L., Dykstra, J.E., Adishakti, M.G., Blokland, M., Langenhoff, A.A.M., van der Wal, A., 2019. Diffusion of hydrophilic organic micropollutants in granular activated carbon with different pore sizes. Water Res. 162, 518–527. https://doi.org/10.1016/j.watres.2019.06.012.
Radian, A., Mishael, Y.G., 2008. Characterizing and designing polycation - clay nanocomposites as a basis for imazapyr controlled release formulations. Environ. Sci. Technol. 42, 1511–1516. https://doi.org/10.1021/es7023753.
Ray, J.R., Shabtai, I.A., Teixidó, M., Mishael, Y.G., Sedlak, D.L., 2019. Polymer-clay composite geomedia for sorptive removal of trace organic compounds and metals in urban stormwater. Water Res. 157, 454–462. https://doi.org/10.1016/j.watres.2019.03.097.
Schaar, H., Clara, M., Gans, O., Kreuzinger, N., 2010. Micropollutant removal during biological wastewater treatment and a subsequent ozonation step. Environ. Pollut. 158, 1399–1404. https://doi.org/10.1016/j.envpol.2009.12.038.
Schapira, M., Manor, O., Golan, N., Kalo, D., Mordehay, V., Kirshenbaum, N., Goldsmith, R., Chefetz, B., Paltiel, O., 2020. Involuntary human exposure to carbamazepine: a cross-sectional study of correlates across the lifespan and dietary spectrum. Environ. Int. 143, 105951. https://doi.org/10.1016/j.envint.2020.105951.
Schreiber, B., Brinkmann, T., Schmalz, V., Worch, E., 2005. Adsorption of dissolved organic matter onto activated carbon—the influence of temperature, absorption wavelength, and molecular size. Water Res. 39, 3449–3456. https://doi.org/10.1016/J.WATRES.2005.05.050.
Sebastiani, E.G., Snoeyink, V.L., Angelotti, R.W., 1994. Thermal regeneration of spent and acidwashed GAC from the Upper Occoquan Sewage Authority. Water Environ. Res. 66, 199–205. https://doi.org/10.2175/WER.66.3.4.
Shabtai, I.A., Mishael, Y.G., 2018. Polycyclodextrin–clay composites: regenerable dual-site sorbents for bisphenol a removal from treated wastewater. ACS Appl. Mater. Interfaces 10, 27088–27097. https://doi.org/10.1021/acsami.8b09715.
Shabtai, I.A., Lynch, L.M., Mishael, Y.G., 2021. Designing clay-polymer nanocomposite sorbents for water treatment: a review and meta-analysis of the past decade. Water Res. https://doi.org/10.1016/j.watres.2020.116571.
Shenker, M., Harush, D., Ben-Ari, J., Chefetz, B., 2011. Uptake of carbamazepine by cucumber plants–a case study related to irrigation with reclaimed wastewater. Chemosphere 82, 905–910. https://doi.org/10.1016/j.chemosphere.2010.10.052.
Shin, J., Kwak, J., Lee, Y.G., Kim, S., Choi, M., Bae, S., Lee, S.H., Park, Y., Chon, K., 2021. Competitive adsorption of pharmaceuticals in lake water and wastewater effluent by pristine and NaOH-activated biochars from spent coffee wastes: contribution of hydrophobic and π-π interactions. Environ. Pollut. 270, 116244. https://doi.org/10.1016/j.envpol.2020.116244.
Shon, H.K., Vigneswaran, S., Snyder, S.A., 2006. Effluent Organic Matter (EfOM) in wastewater: constituents, effects, and treatment. Crit. Rev. Environ. Sci. Technol. 36, 327–374. https://doi.org/10.1080/10643380600580011.
Siemens, J., Huschek, G., Siebe, C., Kaupenjohann, M., 2008. Concentrations and mobility of human pharmaceuticals in the world's largest wastewater irrigation system, Mexico City-Mezquital Valley. Water Res. 42, 2124–2134. https://doi.org/10.1016/j.watres.2007.11.019.
Thompson, M.L., McBride, J.F., Horton, R., 1985. Effects of drying treatments on porosity of soil materials. Soil Sci. Soc. Am. J. 49, 1360–1364. https://doi.org/10.2136/sssaj1985.03615995004900060006x.
Unuabonah, E.I., Taubert, A., 2014. Clay-polymer nanocomposites (CPNs): adsorbents of the future for water treatment. Appl. Clay Sci. https://doi.org/10.1016/j.clay.2014.06.016.
Valderrama, C., Gamisans, X., de las Heras, X., Farrán, A., Cortina, J.L., 2008. Sorption kinetics of polycyclic aromatic hydrocarbons removal using granular activated carbon: Intraparticle diffusion coefficients. J. Hazard. Mater. 157, 386–396. https://doi.org/10.1016/j.jhazmat.2007.12.119.
Van Der Bruggen, B., Vandecasteele, C., 2003. Removal of pollutants from surface water and groundwater by nanofiltration: overview of possible applications in the drinking water industry. Environ. Pollut. 122, 435–445. https://doi.org/10.1016/S0269-7491(02)00308-1.
Wu, X., Ernst, F., Conkle, J.L., Gan, J., 2013. Comparative uptake and translocation of pharmaceutical and personal care products (PPCPs) by common vegetables. Environ. Int. 60, 15–22. https://doi.org/10.1016/j.envint.2013.07.015.
Yu, J., Lv, L., Lan, P., Zhang, S., Pan, B., Zhang, W., 2012. Effect of effluent organic matter on the adsorption of perfluorinated compounds onto activated carbon. J. Hazard. Mater. 225–226, 99–106. https://doi.org/10.1016/j.jhazmat.2012.04.073.
Zietzschmann, F., Müller, J., Sperlich, A., Ruhl, A.S., Meinel, F., Altmann, J., Jekel, M., 2014. Rapid Small-Scale Column Testing of Granular Activated Carbon for Organic Micro-Pollutant Removal in Treated Domestic Wastewater. https://doi.org/10.2166/wst.2014.357.
Zusman, O.B., Kummel, M.L., De la Rosa, J.M., Mishael, Y.G., 2020. Dissolved organic matter adsorption from surface waters by granular composites versus granular activated carbon columns: An applicable approach. Water Res. 181, 115920. https://doi.org/10.1016/j.watres.2020.115920.